ON VORTEX GENERATING JETS

Zia U. Khan
A.T. Kearney, Inc.
153 East 53rd Street, New York NY 10022, USA

James P. Johnston
Department of Mechanical Engineering
Stanford University
Stanford, CA 94305-3030, USA

ABSTRACT

Vortex Generating Jets (VGJs) are jets that pass through a wall and into a crossflow to create a dominant streamwise vortex that remains embedded in the boundary layer over the wall. The VGJ is characterized by its pitch and skew angles (Φ and Θ), and the velocity ratio between the jet and the crossflow (VR).

The VGJ configuration of Φ=30°, Θ=60° for VR=1.0 has been identified as that which produces the strongest vortex. Three component Laser Doppler Velocimetry (LDV) data for this particular configuration demonstrate many interesting features of the flow. Mean velocity data show a deficit of streamwise momentum in the core of the vortex, thinning of the boundary layer on the downwash side of the vortex, and thickening of the boundary layer on the upwash side. Plots of the turbulent kinetic energy and the turbulent shear stress <uv> show that the turbulent structure of the boundary layer is grossly disturbed by the presence of the vortex. The turbulent transport of the turbulent kinetic energy shows the possibility for a gradient diffusion model in most regions but not not the vortex core.

INTRODUCTION

Figure 1 shows a diagram of the VGJ and its defining parameters. The jet passes through a circular hole (the jet-hole) of diameter D through a wall over which the crossflow produces a turbulent boundary layer. The angle between the jet-hole centerline and the wall is the pitch angle, Φ. The angle between the projection of the centerline onto the wall and the crossflow (streamwise) direction is the skew angle, Θ. Because the jet is pitched with respect to the wall, the opening at the wall surface (the jet-orifice) is an ellipse. The skew angle can also be thought of as the angle between the major axis of the ellipse and the streamwise direction.

The origin of the coordinate system is located at the center of the jet-orifice. The streamwise direction is denoted by the x-coordinate; the direction normal to the wall by the y-coordinate; and the spanwise direction along the wall by the z-coordinate.

VGJs are particularly important to two engineering applications. The first application is boundary layer separation control. Boundary layers will separate when the streamwise momentum at the surface of the wall, and hence the wall shear stress, decrease to zero. The dominant streamwise vortex, which remains embedded in the turbulent boundary layer, helps to prevent this by sweeping fluid with high streamwise momentum from the freestream in towards the wall.

The second application is film cooling, in which jets are used to provide a protective layer of cool fluid over a surface exposed to hot gases. In this case, the sweeping of the hot freestream fluid towards the wall effected by the embedded vortex is not desirable.

VGJs relate to two canonical flows that have been studied in the past. The first flow is the normal jet in crossflow. Research in this flow has been extensively reviewed by Margason (1983) and recently discussed by Fric and Roshko (1994) and Kelso et al. (1996). Shi et al. (1991) discussed the vorticity dynamics in the near field of the normal jet that create the symmetric counter-rotating vortex pair. Khan (1999) showed that these same vorticity dynamics give rise to the dominant vortex of the VGJ. Andreopoulos and Rodi (1984) provided detailed turbulence measurements of the normal jet in crossflow.

The second flow, and one that is more relevant to the results being presented in this paper, is the embedded vortex in a turbulent boundary layer. Bradshaw (1987) reviewed turbulent flows with streamwise vorticity, including flows with vortices aligned in the streamwise direction. It was noted that most measurements show

high values of turbulence in the core of the vortex. Since turbulence should be suppressed in the viscous core, these measurements are probably indicative of *vortex meandering*, or the wandering of the vortex in the measurement plane. We will return to this phenomena in the discussion of our own data. Shabaka et al. (1985), Pauley (1988), Westphal and Mehta (1989), and Cutler and Bradshaw (1993a, 1993b) all performed experiments with either a single vortex or arrays of vortices embedded in turbulent boundary layers.

In addition to research in these two canonical flows, considerable work has been recently performed in VGJ flows themselves. Lin et al. (1990) reviewed various passive and active methods for controlling 2D turbulent separated flows. It was found that VGJs were highly effective compared to the more traditional solid vortex generators (generally tabs mounted on the surface) which have an additional drag penalty. Johnston and Nishi (1990) studied spanwise arrays of VGJs and demonstrated that they were effective in reducing stalled regions of the flow. Compton and Johnston (1992) studied the flow from a single VGJ and confirmed that the vortex produced by the VGJ resembled that produced by solid vortex generators, but decayed somewhat faster downstream. Nishi et al. (1995) demonstrated that VGJs could enhance the pressure recovery in a diffuser. Honami et al. (1994) looked at VGJs for use in film cooling applications and found that the asymmetry of the flow reduced the film-cooling effectiveness of the jets. More recently, Zhang (1998) performed detailed LDV measurements that characterized the distributions of the turbulent stresses in the flow.

EXPERIMENT

The research was performed using a low-speed free surface water channel. The jet could be mounted on the test wall inside the water channel. The freestream velocity for the crossflow was Ue=0.2 m/s. At the jet location, the boundary layer had a Reynolds number based on momentum thickness of 1100. The Reynolds number of the jet, based on jet-hole diameter (D) and mean jet speed, was 5000.

The measurements were made using a three-component Laser Doppler Velocimetry system that was composed of one two-component probe and one one-component probe. The probes were orthogonal to each other with intersecting measuring volumes. Each probe was used as the other probe's receiving optics. This guaranteed that the measuring volumes from the two probes were coincident for all of the measurements. The measuring volume was spherical and approximately 2 viscous lengths in diameter.

Further details of the experimental techniques can be found in Khan (1999).

RESULTS AND DISCUSSION

In our experiments, described in Khan (1999), several VGJ configurations were studied at several downstream locations. In this paper, we will only examine the results from one configuration (Φ=30° and Θ=60°) at one velocity ratio (VR=1.0) and at one downstream location (x/D=20). This geometrical configuration produced the strongest dominant vortex at VR=1.0.

The distributions of the mean velocities, mean streamwise vorticity, turbulent kinetic energy, and <uv> shear stress distributions will be presented in this paper. All quantities have been normalized by the freestream velocity, Ue, and the jet-hole diameter, D.

Mean Velocities

The mean velocity distribution is shown in Figure 2. The horizontal axis is the spanwise direction, (z/D), and the vertical axis is the wall-normal, (y/D). The contours represent the streamwise velocity U. The streamwise direction in this and subsequent plots is into the page, away from the reader. The vectors represent the secondary flow (V,W). A reference vector with velocity magnitude 0.2 Ue is shown at the top of the plot.

The thinning of the boundary layer on the downwash side of the vortex and the thickening of the boundary layer on the upwash side are both clear from the streamwise velocity contours. The secondary flow is quite strong near the wall, reaching velocity magnitudes of up to 0.2 Ue. There is a streamwise velocity deficit in the vortex core, where U is only 0.75.

The secondary flow streamlines are somewhat oval-shaped in the core region. This may result from vortex meandering in the spanwise direction, or it may result simply from the "flattening" of the wall which may be represented by a potential flow model with an image vortex to represent the wall. Flow visualization at these experimental conditions revealed that the vortex incurs random spanwise movements. This suggests that vortex meander is the more likely cause of oval-shaped secondary streamlines.

Mean Streamwise Vorticity

The mean streamwise vorticity distribution is shown in Figure 3. There are two distinct vortical regions: the negative region associated with the vortex and the positive region associated with the spanwise shear layer created by the secondary flow over the wall.

The negative vorticity contours appear to be twin-lobed. This shape is the result of the oval-shaped secondary flow streamlines. The positive vorticity is located primarily in the near-wall upwash region.

Turbulent Kinetic Energy

The turbulent kinetic energy, $q^2/2$, is shown in Figure 4 (as contours of q^2). The turbulence levels in the near-wall upwash region are quite high because the secondary flow is convecting highly turbulent flow from very close to the wall upwards. The turbulence levels in the core are also quite high. The most likely reason for this is vortex meandering, in which the moving vortex creates artificial turbulence through the Reynolds averaging of an unsteady flow.

The turbulent transport of q^2 can be characterized by the transport vectors (V_q, W_q) defined as:

$$V_q = \frac{< q^2 v >}{q^2}, \quad W_q = \frac{< q^2 w >}{q^2}$$

Figure 4 shows the vectors of the turbulent transport superimposed over the contours of q^2. For most regions, the vectors are perpendicular to the contours and their magnitude is correlated to the relative proximity of adjacent contours. Both these phenomena imply that in these regions gradient modeling of the turbulent transport of q^2 may be appropriate.

However, in the core of the vortex this is no longer the case. Here, it is clear that the vectors are not perpendicular to the contours. In fact it appears that the vectors are tangential to the contours and are oriented in a direction opposite that of the secondary flow. This strange behaviour can also be seen in the data of Pauley (1988).

The production of turbulent kinetic energy can be determined if the slender flow approximation (that gradients in the x-direction are negligible) is used. The distribution of q^2 production is shown in Figure 5. The production is strongest near the wall and in the upwash region close to the wall. Elsewhere it is smaller.

Turbulent Shear Stress

Although the three component LDV system allows us to measure all three shear stresses, in this paper only the most important component, <uv>, will be discussed.

Figure 6 shows the distribution of <uv>. There are three principal regions: negative <uv> at the top of the vortex core, positive <uv> below the vortex core, and negative <uv> in the thinned and thickened portions of the boundary layer. The positive values for <uv>, which is normally negative in wall-bounded shear flows, arise from the fact that U decreases with increasing y in the region below the vortex. The negative values for <uv> on top of the vortex arise from the fact that U increases from the low speed vortex core region to the freestream with increasing y.

The correlation coefficient for <uv>, Ruv, is shown in Figure 7. It can be seen that the negative region of <uv> on top of the vortex, and to a lesser degree the other two regions, are highly correlated. This means that the <uv> distributions reflect correlated stresses and are not simply the result of augmented values of <uu> or <vv> due the presence of the embedded vortex in the boundary layer.

CONCLUSIONS

The principal conclusions of this paper are:

- The VGJ does produce a dominant vortex that remains embedded in the boundary layer.
- The secondary flow of the vortex has the effect of thinning the boundary layer on the downwash side and thickening it on the upwash side. The core of the vortex has a streamwise momentum deficit.
- The vortex enhances the turbulence levels in the boundary layer.
- The turbulent transport of turbulent kinetic energy may be represented by a turbulent diffusion model, except in the vortex core region.
- The production of turbulent kinetic energy occurs close to the wall.
- The shear stress <uv> distribution of the boundary layer is distorted by the vortex, with even a region of positive <uv> being created. These stresses are well correlated and are not simply the result of augmented levels of <uu> and <vv>.

REFERENCES

Andreopoulos, J., and Rodi, W., 1984, "Experimental Investigation of Jets in Crossflow," *Journal of Fluid Mechanics*, Vol. 138, pp. 93-127.

Bradshaw, P., 1987, "Turbulent Secondary Flow," *Annual Review of Fluid Mechanics*, Vol. 19, pp. 53-74.

Compton, D. A., and Johnston, J. P., 1992, "Streamwise Vortex Production by Pitched and Skewed Jets in a Turbulent Boundary Layer," *AIAA Journal*, Vol. 30, pp. 640-647.

Cutler, A. D., and Bradshaw, P., 1993a, "Strong Vortex/Boundary Layer Interactions. Part I. Vortices High," *Experiments in Fluids*, Vol. 14, pp. 321-332.

Cutler, A. D., and Bradshaw, P., 1993b, "Strong Vortex/Boundary Layer Interactions. Part II. Vortices Low," *Experiments in Fluids*, Vol. 14, pp. 393-401.

Fric, T. F., and Roshko, A., 1994, "Vortical Structure in the Wake of a Transverse Jet," *Journal of Fluid Mechanics*, Vol. 279, pp. 1-47.

Honami, S., Shizawa, T., and Uchiyama, A., 1994, "Behavior of the Laterally Injected Jet in Film Cooling: Measurements of Surface Temperature and Velocity/Temperature Field within the Jet," ASME *Journal of Turbomachinery*, Vol. 116, pp. 106-112.

Johnston, J. P., and Nishi, M., 1990, "Vortex Generator Jets - Means for Flow Separation Control," *AIAA Journal*, Vol. 28, pp. 429-436.

Kelso, R. M., Lim, T. T., and Perry, A. E., 1996 "An Experimental Study of Round Jets in Cross-Flow," *Journal of Fluid Mechanics*, Vol. 306, pp. 111-144.

Khan, Z. U., 1999, "On the Dominant Vortex Produced by a Pitched and Skewed Jet in Crossflow," Ph.D. Thesis, Stanford University, Stanford, CA.

Lin, J. C., Howard, F. G., and Bushnell, D. M., 1990, "Investigation of Several Passive and Active Methods for Turbulent Flow Separation Control," *AIAA 90-1598.*

Pauley, W. R. , 1988, "The Fluid Dynamics and Heat Transfer Effects of Streamwise Vortices Embedded in a Turbulent Boundary Layer", Ph.D. Thesis, Stanford University, Stanford, CA.

Shabaka, I. M. M. A., Mehta, R. D., and Bradshaw, P., 1985, "Longitudinal Vortices Embedded in Turbulent Boundary Layers. Part 1. Single Vortex," *Journal of Fluid Mechanics*, Vol. 155, pp. 37-57.

Shi, Z., Wu, J. Z., and Wu, J. M., 1991, "Symmetric and Asymmetric Jets in a Uniform Crossflow," *AIAA 91-0722.*

Westphal, R. V., and Mehta, R. D., 1989, "Interaction of an Oscillating Vortex with a Turbulent Boundary Layer," *Experiments in Fluids*, Vol. 7, pp. 405-411.

Zhang, X., 1998, "Turbulence Measurements of a Longitudinal Vortex Generated by an Inclined Jet in a Turbulent Boundary Layer," ASME *Journal of Fluids Engineering,* Vol. 120, pp. 1-7.

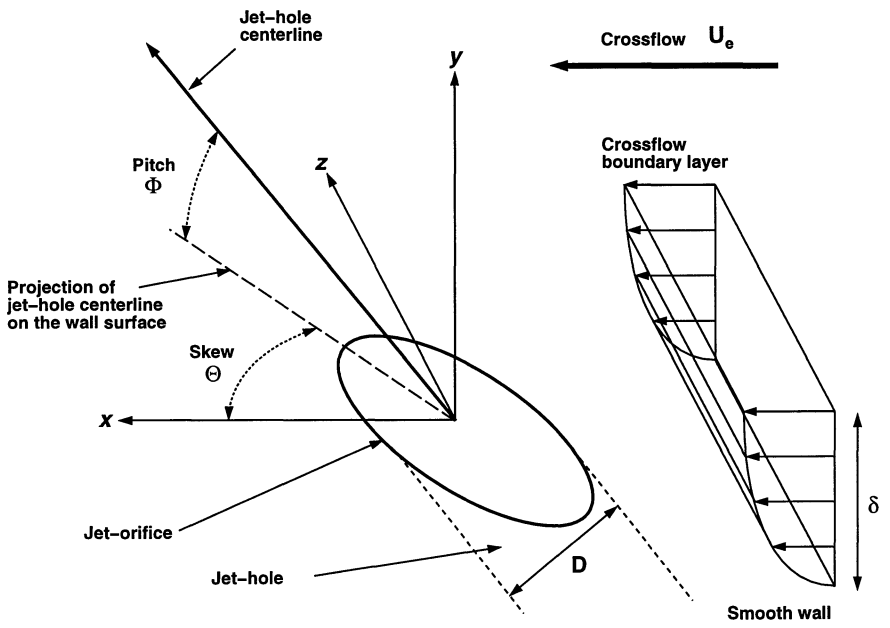

Figure 1: VGJ defining parameters. The origin of the coordinate system is located at the center of the jet-orifice. Crossflow is right to left.

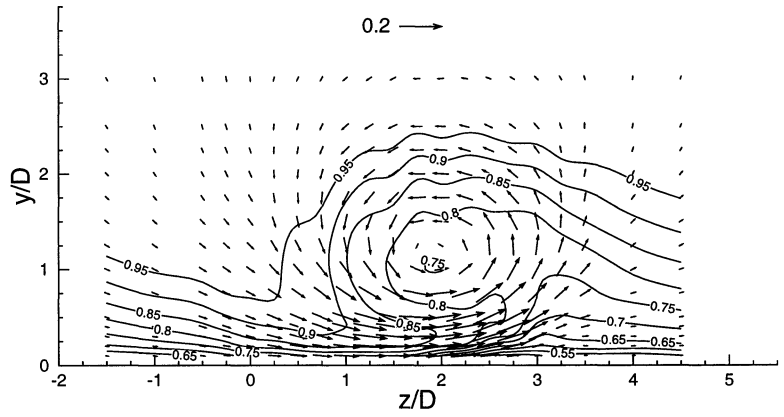

Figure 2: Distribution of mean velocities. Contours are for streamwise velocity U; vectors are for secondary flow (V,W). Reference vector is shown at top of plot for vector of magnitude 0.2 U_e.

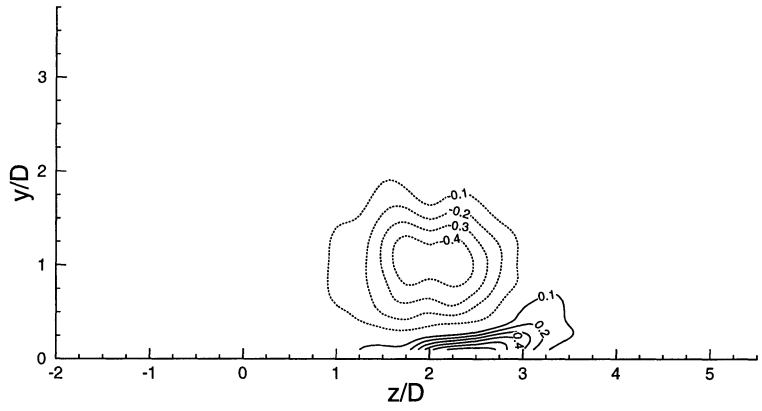

Figure 3: Distribution of mean streamwise vorticity. Dashed lines indicate negative values.

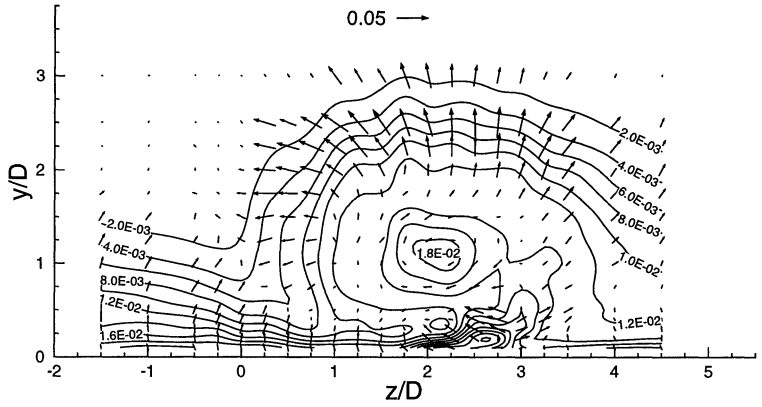

Figure 4: Distribution of q^2 (contours) and turbulent transport of q^2 (vectors). Reference vector at top.

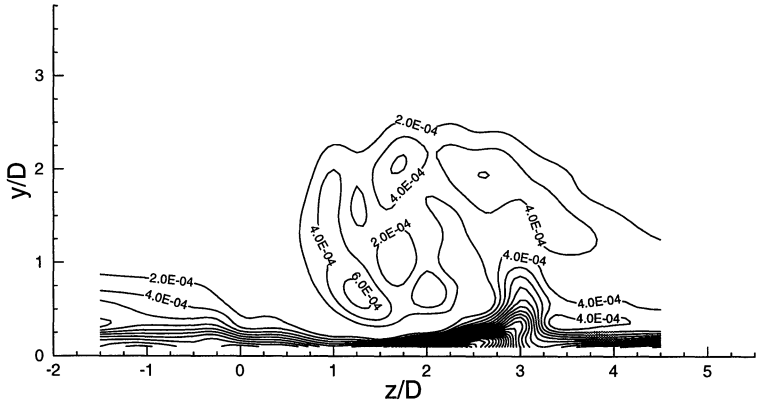

Figure 5: Distribution of turbulent kinetic energy production.

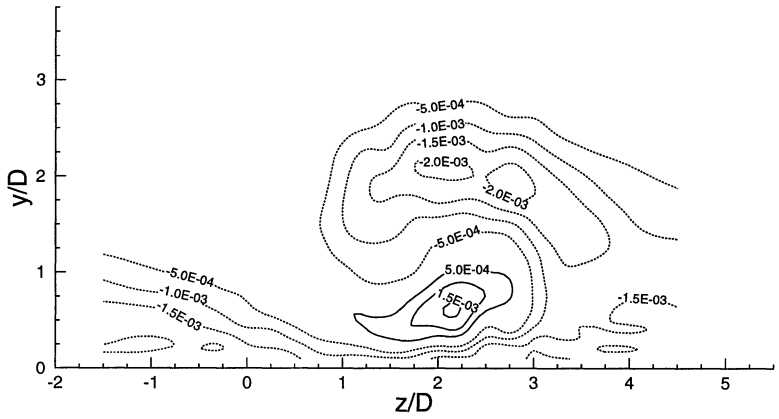

Figure 6: Distribution of $< uv >$.

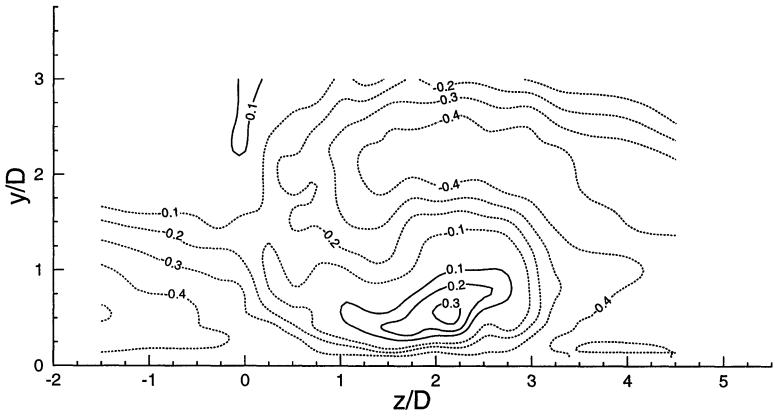

Figure 7: Distribution of R_{uv}.